Half-Lives of the 2+ Rotational States in Dy^{158} and Gd^{158} and Several Other Half-Life Measurements for Deformed Nuclei*

E. G. Funk, H. J. Prask,† and J. W. Mihelich
University of Notre Dame, Notre Dame, Indiana
(Received 20 August 1965)

The half-lives of the 99.1-keV level in Dy^{158} and the 79.6-keV level in Gd^{158} have been measured to be 1.64 ± 0.08 nsec and 2.47 ± 0.10 nsec, respectively, using a source of Tb^{158} (150 yr) and a time-to-amplitude converter circuit. In addition, the following half-lives were measured: 86.8-keV state in Dy^{160}, 2.02 ± 0.09 nsec; 84.2-keV state in Yb^{170}, 1.56 ± 0.08 nsec; 76.5-keV state in Yb^{174}, 1.74 ± 0.09 nsec; 100.1-keV state in W^{182}, 1.35 ± 0.7 nsec; 1289-keV state in W^{182}, 1.06 ± 0.05 nsec. A compilation of the more recent data on first excited state half-lives, $B(E2)$ values, and deformation parameters is presented for the even-even rotational nuclei in the region $Z=60$–68. A comparison is made between values determined from half-life and Coulomb-excitation measurements.

I. INTRODUCTION

The direct measurement of half-lives of first excited 2+ states for rotational nuclei and Coulomb-excitation experiments are complementary methods for obtaining reduced $E2$ transition probabilities and nuclear deformation parameters. These experimental data provide a sensitive test for the various models and theories proposed for rotational nuclei.

This paper is concerned mainly with delayed-coincidence measurements of the half-lives of the first excited states of Dy^{158} and Gd^{158}. These measurements were carried out using a time-to-amplitude converter (TAC) circuit and a source of long-lived Tb^{158} ($\sim$150 yr) which decays by electron capture to Gd^{158} and by beta decay to Dy^{158}.[1]

In addition, the results of several other half-life determinations for states in deformed nuclei are reported. All of these have been previously measured by other investigators. A compilation of the more recent data on first excited state half-lives, $B(E2)$ values, and deformation parameters is presented for the Nd, Sm, Gd, Dy, and Er rotational nuclei. A comparison is made between results obtained from lifetime and Coulomb-excitation measurements.

II. EXPERIMENTAL APPARATUS

The delayed-coincidence apparatus employed Pilot B scintillators and RCA 6342 A photomultipliers (high voltage $\approx$2200 V).[2] In every case a thin scintillator (0.015 to 0.030 in.)$\times$1 in. was used for low-energy conversion-electron detection. The other detector utilized either a 1-in.$\times$1-in. crystal for γ-ray detection or a $\frac{1}{16}$-in.$\times$1-in. crystal for β-ray detection. The source material was deposited on 1 mg/cm^2 aluminized Mylar which was then mounted about $\frac{1}{8}$ in. from the thin scintillator. A light-tight housing having a thin end window covered this source-detector assembly. The second detector was mounted in 180° geometry about $\frac{1}{4}$ in. from the source.

The voltage pulses from the detectors were amplified by two-stage fast amplifiers (employing type 6688 pentodes) and then limited by 404 A limiters of the Simms type.[3] The time-to-amplitude converter was a 6BN6 circuit.[4] No pulse height compensation or pile-up rejection circuits were used for these measurements. The time calibration for each measurement was obtained by inserting a length of RG-63U cable whose delay had been measured with a fast pulser and sampling oscilloscope. This calibration was carried out in a manner which eliminated any error due to cable-connector effects.

III. RESULTS

A partial decay scheme for Tb^{158} (150 yr)[1,5] is shown in the insert in Fig. 1. Intensities (based on 100 total Tb^{158} decays) are given for the higher energy gamma rays. The half-life data for the 80 keV state in Gd^{158} are shown as curve A in Fig. 1(a), and a prompt curve obtained with Co^{60} is shown as curve B. The energy-selection gates for this run are shown in Fig. 2. (Identical gates were used for the Co^{60} prompt curve.) The gates were set on the 80-L conversion electrons and from $\approx$600 to 800 keV on the Compton distribution for the $\approx$950-keV gamma rays. A beta-ray absorber of 400 mg/cm^2 Al was interposed between the source and gamma-ray detector. Four separate runs of about 10 h each were carried out, and the data were combined after adjustment for a slight gain shift (the variation in peak position was no greater than one channel). A weighted least-squares analysis of the combined data yielded a value of $T_{1/2}=2.47\pm0.10$ nsec, where the quoted error includes a reasonable

* Work supported in part by the U. S. Atomic Energy Commission.
† Now at U. S. Army Materials Research Agency, Watertown, Massachusetts.
[1] F. Schima, E. G. Funk, Jr., and J. W. Mihelich, Nucl. Phys. 63, 305 (1965).
[2] E. G. Funk, Jr., H. J. Prask, F. Schima, J. McNulty, and J. W. Mihelich, Phys. Rev. 129, 757 (1963).
[3] P. C. Simms, Rev. Sci. Instr. 32, 894 (1961).
[4] R. E. Green and R. E. Bell, Nucl. Instr. 3, 127 (1958).
[5] *Nuclear Data Sheets*, compiled by K. Way *et al.* (Printing and Publishing Office, National Academy of Sciences—National Research Council, Washington 25, D. C.).

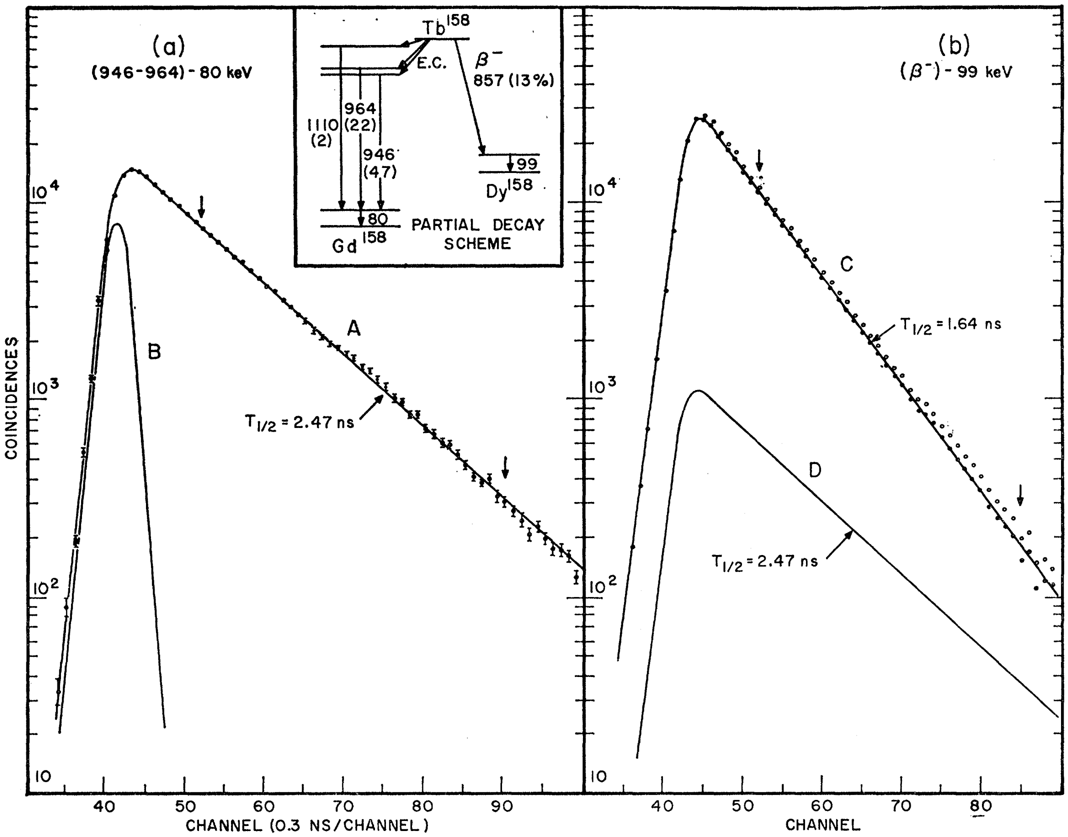

FIG. 1. (a) Curve A shows the Gd^{158} half-life curve obtained when gating on (946–964)-keV gamma rays and 80-L conversion electrons, and curve B shows the Co^{60} prompt curve. A partial decay scheme for Tb^{158} is shown in the insert. (b) Curve C (open circles) shows the half-life curve obtained when gating on the beta spectrum (end-point 857 keV) and 99-L keV conversion electrons. Curve D shows the contribution of (946–964)-keV γ-(80-L)e^- coincidences to curve C (open circles), obtained by absorbing the beta particles. The Dy^{158} half-life data is the difference between the data of C (open circles) and curve D, and is shown as the solid dots (curve C).

uncertainty in the time calibration. Only the data points bracketed by the arrows in Fig. 1(a) were included in the least-squares fit.

In order to measure the half-life of the 99-keV state in Dy^{158}, it is necessary to gate on the beta spectrum (end-point 857 keV) and the 99-L conversion electrons. Since some 946- and 964-keV gamma rays are detected in the beta detector and the 99-L electrons are not resolved from the 80-L electrons, the resultant half-life curve contains a contribution from the 2.47 nsec half-

TABLE I. Results of half-life measurements.

Nucleus	Source	Level energy[a] (keV)	Energy selection gates (keV)	Measured $T_{1/2}$ (nsec)	Other $T_{1/2}$ results[f] (nsec)
Gd^{158}	Tb^{158} (150 yr)	79.6	($\approx$710γ) (80-Le^-)[b]	2.47$\pm$0.10	2.34(10)[g]
Dy^{158}	Tb^{158} (150 yr)	99.3	($\approx$400β) (99-Le^-)[c]	1.64$\pm$0.08	
Dy^{160}	Tb^{160} (72 day)	86.8	($\approx$950γ) (87-Le^-)	2.02$\pm$0.09	1.92(5), 1.99(5), 2.059(16)[h]
Yb^{170}	Tm^{170} (127 day)	84.2	($\approx$500β) (84-Le^-)	1.56$\pm$0.08	1.57(5), 1.61(6), 1.47(4)[i]
Yb^{174}	Lu^{174} ($\approx$1300 day)	76.5	($\approx$1020γ) (77-Le^-)	1.74$\pm$0.09	1.91(20), 1.80(10)[j]
W^{182}	Ta^{182} (115 day)	100.1	($\approx$900γ) (100-Le^-)[d]	1.35$\pm$0.07	1.43(4), 1.37(2) 1.39(3), 1.47(9)[k]
		1289	($\approx$90β) ($\approx$900γ)[d] ($\approx$130β) ($\approx$900γ)[e]	1.06$\pm$0.05	1.02(7), 1.03(3) 1.03(3), 1.04(3)[l]

[a] From Ref. 5.
[b] Gates centered at $\approx$710 keV on Compton edge of 950-keV gamma rays and at energy of L conversion electrons from 80-keV transition.
[c] See text for further explanation.
[d] Gate contained both 100-L conversion electrons and betas of $\approx$90 keV. The half-lives of both the 100- and 1289-keV states appear on curve D, of Fig. 3.
[e] These gate settings yield only the half-life of the 1289-keV state (curve E, Fig. 3).
[f] All quoted results are direct half-life measurements. Errors are given in parentheses.
[g] See Ref. 6.
[h] See Refs. 7, 8, and 9.
[i] See Refs. 10, 11, and 7.
[j] See Refs. 6 and 12.
[k] See Refs. 6, 13, 14, and 15.
[l] See Refs. 16, 17, 14, and 15.

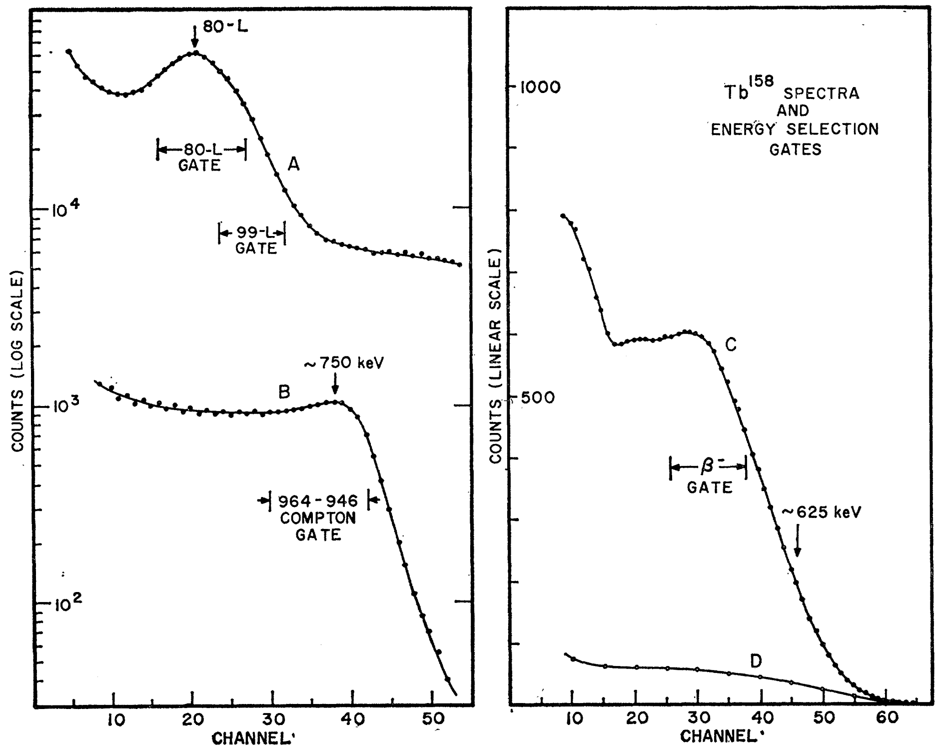

FIG. 2. Curve A shows the Tb^{158} conversion-electron spectrum observed with the $\frac{1}{32}$″ Pilot B scintillator, curve B the gamma-ray spectrum from the 1-in.×1-in. scintillator, curve C the beta spectrum from the $\frac{1}{16}$-in. scintillator, and curve D the gamma-ray spectrum from the $\frac{1}{16}$-in. scintillator with frontal Al absorber. The energy selection gates are shown for each case.

life in Gd^{158}. A $\frac{1}{16}$-in. thick Pilot B beta detector was chosen, minimizing the gamma-ray contribution but giving a reasonable efficiency for beta detection.

Two half-life measurements were carried out, one with no absorber (actually $\approx$10-mg/cm² Al light reflector) between the source and beta detector and the other with a 400-mg/cm² Al absorber. The half-life curve obtained with the absorber (curve D of Fig. 1) showed a 2.5-nsec slope as expected. These data, suitably normalized to equal counting time, were

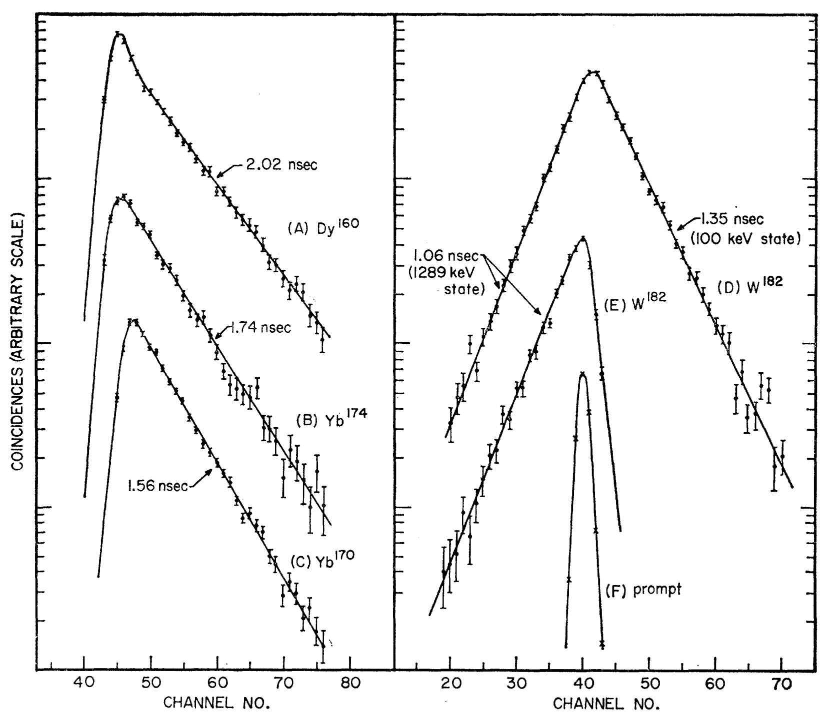

FIG. 3. Half-life curves obtained for the first 2+ states in Dy^{160}, Yb^{174}, Yb^{170}, W^{182}, and the 1289-keV state in W^{182}. A prompt curve is also shown. Details are given in Table I.

TABLE II. $T_{1/2}$, energies, $B(E2)$, Q_0 values, and deformation parameters for the first 2+ states in Nd, Sm, Gd, Dy, and Er nuclei.

Nuclide	Level[a] energy (keV)	E_4/E_2[a]	$T_{1/2}$[b] (nsec)	α_T[c]	τ_γ[d] (nsec)	$B(E2;2\rightarrow 0)\downarrow_\tau$[e] ($e^2\times 10^{-48}$ cm^4)	$B(E2;2\rightarrow 0)\downarrow_{CE}$[f] ($e^2\times 10^{-48}$ cm^4)	Q_0[d] (10^{-24} cm^2)	β[d]	ϵ[d]	$\mathcal{I}/\mathcal{I}_{rig}$[d]	$(\mathcal{I}/\mathcal{I}_{rig})/\beta^2$	$[B(E2)\downarrow\times E]$[d]
$_{60}Nd_{90}^{150}$	131	2.98	1.54(7)[g]	0.857	4.12	0.51(3)	0.53(2)	5.07(12)	0.263	0.233	0.357	5.16	67(4)
$_{62}Sm_{90}^{152}$	121.8	3.01	1.40(3)[h]	1.182	4.40	0.69(2)	0.68(3)	5.88(9)	0.291	0.256	0.373	4.40	84(4)
Sm_{92}^{154}	82.0	3.26	2.74(35)[i]	5.008	23.7	0.92(12)	0.92(4)	6.81(45)	0.332	0.290	0.536	4.87	75(10)
$_{64}Gd_{90}^{154}$	123.1	3.02	1.17(3)[j]	1.215	3.72	0.77(3)	0.69(6)	6.22(10)	0.296	0.260	0.360	4.11	95(4)
Gd_{92}^{156}	89.0	3.24	2.19(4)[k]	3.952	15.6	0.93(3)	0.91(5)	6.84(13)	0.321	0.281	0.484	4.70	83(3)
Gd_{94}^{158}	79.6	3.29	2.41(7)[l]	6.082	24.6	1.03(5)	1.09(5)	7.21(16)	0.335	0.292	0.528	4.71	82(4)
Gd_{94}^{160}	75.3	3.28	2.52(15)[m]	7.517	30.9	1.09(8)	1.16(5)	7.38(26)	0.340	0.296	0.546	4.71	82(6)
$_{66}Dy_{90}^{156}$	138.1	2.94	0.79(7)[n]	0.864	2.12	···	0.76(6)	6.19(15)	0.283	0.250	0.315	3.93	105(9)
Dy_{92}^{158}	99.3	3.19	1.64(8)[o]	2.835	9.05	0.93(5)	0.93(8)	6.83(19)	0.309	0.271	0.426	4.46	92(5)
Dy_{94}^{160}	86.8	3.27	2.00(5)[p]	4.695	16.4	1.00(4)	0.89(6)	7.10(15)	0.318	0.278	0.477	4.72	87(4)
Dy_{96}^{162}	80.7	3.29	2.25(7)[q]	6.235	23.4	1.01(5)	1.02(3)	7.13(17)	0.317	0.277	0.502	5.02	82(4)
Dy_{98}^{164}	73.4	3.30	2.42(24)[r]	9.103	35.2	1.08(11)	1.13(5)	7.37(39)	0.325	0.283	0.540	5.09	83(9)
$_{68}Er_{94}^{162}$	102	3.31	1.39(7)[n]	2.760	7.52	···	0.98(5)	7.01(17)	0.303	0.266	0.399	4.35	100(5)
Er_{96}^{164}	91.5	3.30	1.732(32)[s]	4.157	12.8	0.98(4)	1.01(5)	7.03(13)	0.301	0.265	0.436	4.81	90(4)
			1.6(1)[t]		11.9	1.06(8)		7.32(26)	0.313	0.274	0.435	4.44	97(8)
Er_{98}^{166}	80.6	3.29	1.82(4)[u]	6.878	20.6	1.16(5)	1.13(5)	7.62(16)	0.323	0.282	0.482	4.63	94(4)
Er_{100}^{168}	79.8	3.31	1.91(4)[v]	7.152	22.4	1.12(5)	1.14(4)	7.50(15)	0.316	0.276	0.478	4.78	89(4)
Er_{102}^{170}	78.6	3.32	2.02(10)[n]	7.611	25.1	···	1.09(3)	7.37(15)	0.308	0.270	0.477	5.03	86(3)
$_{70}Yb_{98}^{168}$	88	3.30	1.55(8)[n]	5.338	14.1	···	1.09(5)	7.39(15)	0.303	0.266	0.435	4.74	96(5)

[a] See Ref. 5. E_4/E_2 is the ratio of the energies of the first 4+ and 2+ states.
[b] All values quoted are direct half-life measurements, except for the Dy^{156}, Er^{162}, Er^{170}, and Yb^{168} where $T_{1/2}$ was obtained from Coulomb-excitation results. Errors are given in parentheses.
[c] Total internal conversion coefficients. See text.
[d] Calculated from measured $T_{1/2}$ values except for the cases of Dy^{156}, Er^{162}, Er^{170}, and Yb^{168} where Coulomb-excitation data were used. (Errors in parentheses.)
[e] Calculated from the measured $T_{1/2}$ values. (Errors in parentheses.)
[f] Values obtained from $B(E2)\uparrow$ of Refs. 18 and 19. (Errors in parentheses.)
[g] See Ref. 20.
[h] Average of values from Refs. 7, 21 and 22.
[i] See Ref. 20.
[j] Average of values from Refs. 7, 23, 24, and 25.
[k] Average of values from Refs. 7, 22, and 26.
[l] Average of our value and value from Ref. 6.
[m] See Ref. 20.
[n] Obtained from Coulomb-excitation results of Refs. 18 and 19.
[o] Our result.
[p] Average of our value and values from Refs. 7, 8, and 9.
[q] See Ref. 8.
[r] See Ref. 20.
[s] See Ref. 9.
[t] Average of values from Refs. 7 and 9.
[u] Average of values from Refs. 7, 8, and 27.
[v] Average of values from Refs. 8 and 28.

subtracted from the data obtained with no absorber [open circles in Fig. 1(b)]. The resultant data are shown as curve C in Fig. 1. A least-squares analysis of the data bracketed by the arrows yielded a value of $T_{1/2}=1.64\pm0.08$ nsec, where the error includes calibration uncertainty.

Table I lists the half-life results obtained for the first 2+ states in Dy^{160}, Yb^{170}, Yb^{174}, and W^{182}, and the 1289-keV (2−) state in W^{182}. The half-life data are shown in Fig. 3. The technique employed for these measurements was similar to that described in the previous section. Also included in Table I are the energy selection gates used for each measurement, the results for Gd^{158} and Dy^{158}, and half-life values obtained by other investigators.[6–17]

IV. DISCUSSION

Our value of $T_{1/2}=2.47\pm0.10$ nsec for the 79.6-keV state in Gd^{158} agrees, within errors, with the result of 2.34 ± 0.10 nsec obtained by Birk *et al.*[6] from a $(p,p\gamma)$-delay measurement. The $B(E2)\downarrow$ value resulting from our $T_{1/2}$ measurement is 1.01 ± 0.05. This is in fair agreement with the $B(E2)\downarrow$ value of 1.09 ± 0.05 obtained from the Coulomb-excitation result of Elbek *et al.*[18]

No direct measurements of the half-life of the 99.3-keV state in Dy^{158} have previously been reported, but a value of $B(E2)\downarrow=0.93\pm0.08$ has been obtained by Coulomb excitation.[19] Our half-life result of 1.64 ± 0.08 nsec yields a $B(E2)\downarrow$ value of 0.93 ± 0.05, in excellent agreement with the Coulomb excitation result.

In Table II are listed the energies, half-lives, total internal conversion coefficients (I.C.C.'s), partial γ-ray mean lives τ_γ, $B(E2)$ values and deformation parameters β and ϵ for the Nd, Sm, Gd, Dy, and Er rotational nuclides (Yb^{168} data is presented so as to include all observed $N=98$ nuclides). The half-life values quoted are averages of the more recent accurate measure-

[6] M. Birk, A. E. Blaugrund, G. Goldring, E. Z. Skurnik, and J. S. Sokolowski, Phys. Rev. **126**, 726 (1962).
[7] D. B. Fossan and B. Herskind, Nucl. Phys. **40**, 24 (1963).
[8] A. Li and A. Schwarzschild, Phys. Rev. **129**, 2664 (1963).
[9] T. J. DeBoer, E. W. Ten Napel, and J. Blok, Physica **29**, 1013 (1963).
[10] R. L. Graham, J. L. Wolfson, and R. E. Bell, Can. J. Phys. **30**, 459 (1952).
[11] M. S. El-Nesr and E. Bashandy, Z. Physik **168**, 349 (1962).
[12] J. Jastrzebski, M. Moszyński, K. Pawlak, and K. Stryczniewicz, in *Proceedings of International Conference on Nuclear Physics, Paris, 1964* (National Center of Scientific Research, Paris, 1964), Vol. II, p. 573.
[13] R. P. Scharenberg, J. D. Kurfess, G. Schilling, J. W. Tippie, and P. J. Wolfe, Nucl. Phys. **58**, 658 (1964).
[14] M. Dorikens, O. Segaert, J. Demuynck, and L. Dorikens-Vanpraet, Nucl. Phys. **61**, 33 (1965).
[15] R. Rougny, J. J. Samueli, and A. Sarazin, J. Phys. Radium **25**, 989 (1964).
[16] A. W. Sunyar, Phys. Rev. **93**, 1122 (1954).
[17] S. Gorodetzky, R. Richert, R. Manquenouille, and A. Knipper, Nucl. Instr. **7**, 50 (1960).
[18] B. Elbek, M. C. Olesen, and O. Skilbreid, Nucl. Phys. **19**, 523 (1960).
[19] J. Bjerregard, B. Elbek, O. Hansen, and P. Salling, Nucl. Phys. **44**, 280 (1963).

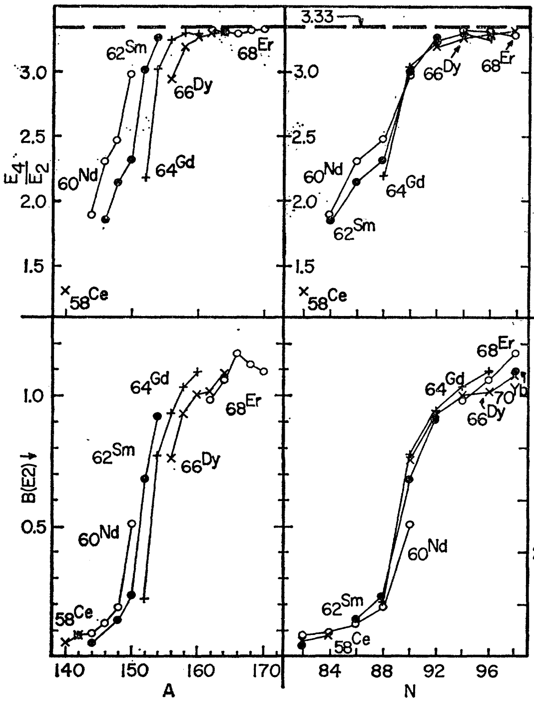

FIG. 4. E_4/E_2 and $B(E2)$ versus A and N for the mass region $A=140-170$ and $N=82-98$. The left-hand scale gives $B(E2)\downarrow$ and the right-hand scale $B(E2)\uparrow$. The lines are drawn connecting the data for nuclei of the same Z. (A consistent set of symbols is used for the various elements in Figs. 4 and 5.) See text for explanation and references.

ments.[6–9,20–28] (References are given in the table.) For all cases except Dy^{156}, Er^{162}, Er^{170}, and Yb^{168}, the $B(E2)\downarrow$ values were calculated from the measured half-life data using the relation

$$[B(E2;2+\rightarrow 0+)\downarrow]^{-1}=1.23\times 10^{-2}E^5(1+\alpha_T)\tau_m,$$

where E is in keV, $B(E2)$ is in units of $e^2\times 10^{-48}$ cm^2, α_T is the total I.C.C., and τ_m is the mean life in sec. The total I.C.C.'s were calculated assuming $\alpha_T=\alpha_K+1.33\alpha_L$. The values of α_K and α_L were accurately interpolated from the tables of Sliv and Band,[29], using a least-squares fitting procedure. The quoted errors for the $B(E2)$ values include a 4% assumed uncertainty in the theoretical α_T. For Dy^{156}, Er^{162}, Er^{170}, and Yb^{168}, the $B(E2)\downarrow$ and $T_{1/2}$ values were calculated from the $B(E2)\uparrow$ found by Coulomb excitation.[18,19] Stelson[30] has recently carried out an analysis of $B(E2)$ values obtained by Coulomb-excitation and half-life measurements. The results indicate that better agreement is obtained using the Sliv and Band I.C.C. values rather than Rose's tables,[31] and that an error of about 4% should be assigned to α_T values from the relation $\alpha_K+1.33\alpha_L$ and the Sliv and Band tables.[29]

It can be seen from Table II that the $B(E2)$ values obtained from half-life and Coulomb-excitation measurements are in good agreement, the worst discrepancies being for Gd^{154} and Dy^{160}. Only for the case of Dy^{160} are the two results outside error limits, and then only slightly. In an earlier comparison of $B(E2)$ results (1960) from the two methods, Elbek *et al.*[18] remarked that the values determined from lifetime measurements were, on the average, about 2% higher than found from Coulomb excitation if the values of Sliv and Band were used for α_T (5% if Rose's values[31] are used). No such trend can be noted from the results in Table II.

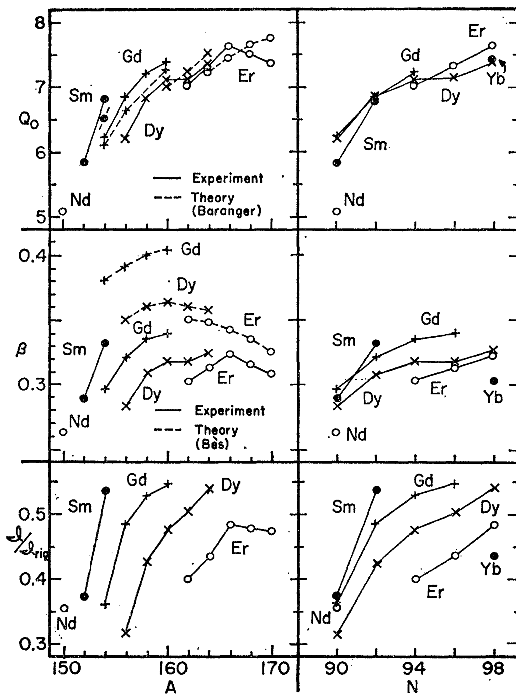

FIG. 5. Q_0, β, and $\mathscr{I}/\mathscr{I}_{\rm rig}$ versus A and N for the rotational region from $A=150-170$ and $N=90-98$. The lines are drawn connecting the data for nuclei of the same Z. See text for explanation and references.

[20] M. Birk, G. Goldring, and Y. Wolfson, Phys. Rev. **116**, 730 (1959).
[21] A. W. Sunyar, Phys. Rev. **98**, 653 (1955).
[22] R. W. Bauer and M. Deutsch, Phys. Rev. **128**, 751 (1962).
[23] T. D. Nainan, Phys. Rev. **123**, 1751 (1961).
[24] R. Stiening and M. Deutsch, Phys. Rev. **121**, 1484 (1961).
[25] J. Burde, M. Rakavy, and G. Rakavy, Phys. Rev. **129**, 2147 (1963).
[26] R. E. Bell and M. H. Jorgensen, Nucl. Phys. **12**, 413 (1959).
[27] R. L. Graham and M. A. Clark, quoted in Ref. 5.
[28] E. Bodenstedt, H. J. Korner, E. Gerdau, J. Radeloff, L. Mayer, K. Auerbach, J. Braunsfurth, and G. Mielken, Z. Physik **170**, 355 (1962).
[29] L. A. Sliv and I. M. Band, *Tables of Internal Conversion Coefficients of Gamma-Rays: I. K-Shell II. L-Shell* (Academy of Sciences, Press, USSR, Moscow-Leningrad, 1956, 1959).

[30] P. Stelson, reported at International Conference on the Internal Conversion Process, Vanderbilt University, Nashville, Tennessee, 1965 (proceedings to be published by Academic Press).
[31] M. E. Rose, *Internal Conversion Coefficients* (North-Holland Publishing Company, Amsterdam, 1958).

The Q_0, β, ϵ, and $\mathcal{I}/\mathcal{I}_{\rm rig}$ values listed in Table II were calculated using the relations[32]

$$B(E2)\downarrow = Q_0^2/16\pi$$

$$Q_0 = [3ZR_0^2/(5\pi)^{1/2}]\beta(1+0.16\beta) = \tfrac{4}{5}ZR_0^2\epsilon(1+\tfrac{1}{2}\epsilon)$$

$$E = (\hbar^2/2\mathcal{I})I(I+1)$$

and

$$\mathcal{I}_{\rm rig} = \tfrac{2}{5}AMR_0^2(1+0.31\beta),$$

where $R_0 = 1.2\times10^{-13}A^{1/3}$ cm, $M = 1.673\times10^{-24}$ g, $B(E2)$ is in units of $e^2\times10^{-48}$ cm^4, and Q_0 in units of 10^{-24} cm^2. The partial gamma-ray mean lives are found from the relation $\tau_\gamma = 1.44T_{1/2}(1+\alpha_T)$. The $B(E2)\downarrow$ values obtained from $T_{1/2}$ measurements were used to calculate Q_0, β, and ϵ, where possible.

Also shown in Table II are values of $B(E2)\downarrow\times E$ and $(\mathcal{I}/\mathcal{I}_{\rm rig})/\beta^2$. It has been pointed out by Grodzins[33] that the product $\tau_\gamma\times E^4$ is approximately a constant for almost all 2+ states in even-even nuclides. Since $B(E2)\downarrow\times E$ is proportional to $(\tau_\gamma\times E^4)^{-1}$, the product $B(E2)\downarrow\times E$ should exhibit the same behavior. The values for the nuclei considered in Table II are seen to be roughly constant with a mean value of 88. The values of $(\mathcal{I}/\mathcal{I}_{\rm rig})/\beta^2$, if errors are considered, are not inconsistent with the relation $\mathcal{I}/\mathcal{I}_{\rm rig} = ({\rm const})\times\beta^2$.

Values of E_{4+}/E_{2+} and $B(E2)\downarrow$ in the transition region and a portion of the rotational region are shown as a function of both mass number A and neutron number N in Fig. 4. The $B(E2)\downarrow$ values for the transition nuclei ($N=82-88$) were obtained from the work of Eccleshall *et al.*,[34] except for Gd^{152}, where the $B(E2)\downarrow$ was obtained from the half-life measurement of Burde *et al.*[35] The $B(E2)\downarrow$ values for the rotational nuclei were taken from Table II.

In Fig. 5 are shown the values of Q_0, β, and $\mathcal{I}/\mathcal{I}_{\rm rig}$ versus A and N for the lower portion of the rotational region ($A=150-170$ and $N=90-98$). The values were taken from Table II. The theoretical predictions for β were obtained from the calculations of Bès and Szymanski,[36] as quoted in the paper of Bjerregard *et al.*[19] Bès and Szymanski calculated the ground-state equilibrium deformations of rare-earth nuclei, using a realistic spacing of the Nilsson single-particle levels and including the effect of the pairing interaction. The theoretical predictions for Q_0 were obtained from the calculations of Baranger[37] as quoted in the paper of Kerman.[38] Baranger included both pairing interaction and quadrupole forces in his calculations. The predictions of Baranger are in good agreement with experiment, and it is apparent that the calculations which include both pairing and quadrupole forces give better agreement with experiment than those which include pairing alone.

ACKNOWLEDGMENTS

The authors wish to thank Dr. Frank Schima for his assistance in the taking and analysis of data and A. Warn-Varnas, J. Sapyta, and J. Jaklevic for carrying out the computer calculations.

[32] K. Alder, A. Bohr, T. Huus, B. Mottelson, and A. Winther, Rev. Mod. Phys. **28**, 432 (1956).

[33] L. Grodzins, Phys. Letters **2**, 88 (1962).

[34] D. Eccleshall, M. J. L. Yates, J. A. Cookson, and J. J. Simpson, in *Proceedings of International Conference on Nuclear Physics, Paris, 1964* (National Center of Scientific Research, Paris, 1964), Vol. 2, p. 469.

[35] J. Burde, M. Rakavy, and S. Ofer, Phys. Rev. **124**, 1911 (1961).

[36] D. R. Bès and Z. Szymanski, Nucl. Phys. **28**, 42 (1961).

[37] M. Baranger, in *Proceedings of International Conference on Nuclear Physics, Paris, 1964* (National Center of Scientific Research, Paris, 1964), Vol. 1, p. 152.

[38] A. K. Kerman, in *Proceedings of International Conference on Nuclear Physics, Paris, 1964* (National Center of Scientific Research, Paris, 1964), Vol. 1, p. 183.